Exhibit K

THE MICROSCOPE • Vol. 69:2, pp 51–69, 2022

The Dispersion Staining Technique and Its Application to Measuring Refractive Indices of Non-opaque Materials, with Emphasis on Asbestos Analysis

Shu-Chun Su, Ph.D.
Technical Expert, National Voluntary Laboratory Accreditation Program
National Institute of Standards and Technology[1]

ABSTRACT

Refractive index (RI) is the most important optical property of non-opaque materials. It is the leading diagnostic optical property of non-opaque materials, especially asbestos minerals. Dispersion staining (DS) has been proven to be the most effective technique with desirable accuracy for the measurement of asbestos minerals' RI using the immersion method by polarized light microscopy (PLM). This paper presents a practical procedure for this measurement. To facilitate the analysis, two comprehensive suites of pre-calculated look-up tables for the conversion of the observed matching wavelength to RI were constructed for the two major types of RI liquids: Cargille Laboratories (Cargille) and Delaware Research Institute of Microscopy and Material Characterization LLC (DRIMMC), respectively, covering the range of RI liquids suitable for analyzing the six regulated asbestos minerals. RI liquid calibration in the absence of an Abbe refractometer is discussed. An alternative solution using Cargille optical glass standards is proposed, and two comprehensive suites of pre-calculated look-up tables for both Cargille and DRIMMC liquids are included, covering the range of RI liquids routinely used in the analysis of the six regulated asbestos minerals.

Keywords: dispersion staining, central stop, annular stop, refractive index, immersion method, polarized light microscopy, refractive index liquid, refractive index liquid calibration, Cargille, DRIMMC, asbestos, non-opaque material, amphibole, amosite, grunerite, crocidolite, riebeckite, tremolite, actinolite, anthophyllite, bulk asbestos sample, conversion table

Scan this QR code to download the four conversion tables (PDF files) for Cargille and DRIMMC RI liquids used in asbestos RI measurement and liquid calibration on www.mccroneinstitute.org[2].

INTRODUCTION

The Asbestos Hazard Emergency Response Act (AHERA), United States Code 15 (1) requires local educational agencies to inspect their school buildings for asbestos-containing building materials, prepare asbestos management plans, and perform asbestos response actions to prevent or reduce asbestos hazards. AHERA defines six asbestiform minerals, i.e., chrysotile, amosite (grunerite), crocidolite (riebeckite), tremolite, actinolite, and anthophyllite to be regulated hazardous asbestos minerals. AHERA also mandates the use of U.S. Environmental Protection Agency (EPA) protocol (2) for the analysis of asbestos content in bulk insulation materials. The analysis uses polarized light microscopy (PLM) to identify and quantify the asbestos minerals in bulk samples, requiring the measurement of six optical properties: color, pleochroism, refractive index (RI), birefringence, extinction, and sign of elongation.

[1] 100 Bureau Drive, Gaithersburg, MD 20899; shuchunsu@gmail.com
[2] https://www.mccroneinstitute.org/v/1624/The-Microscope-Volume-69-Second-Quarter-2022

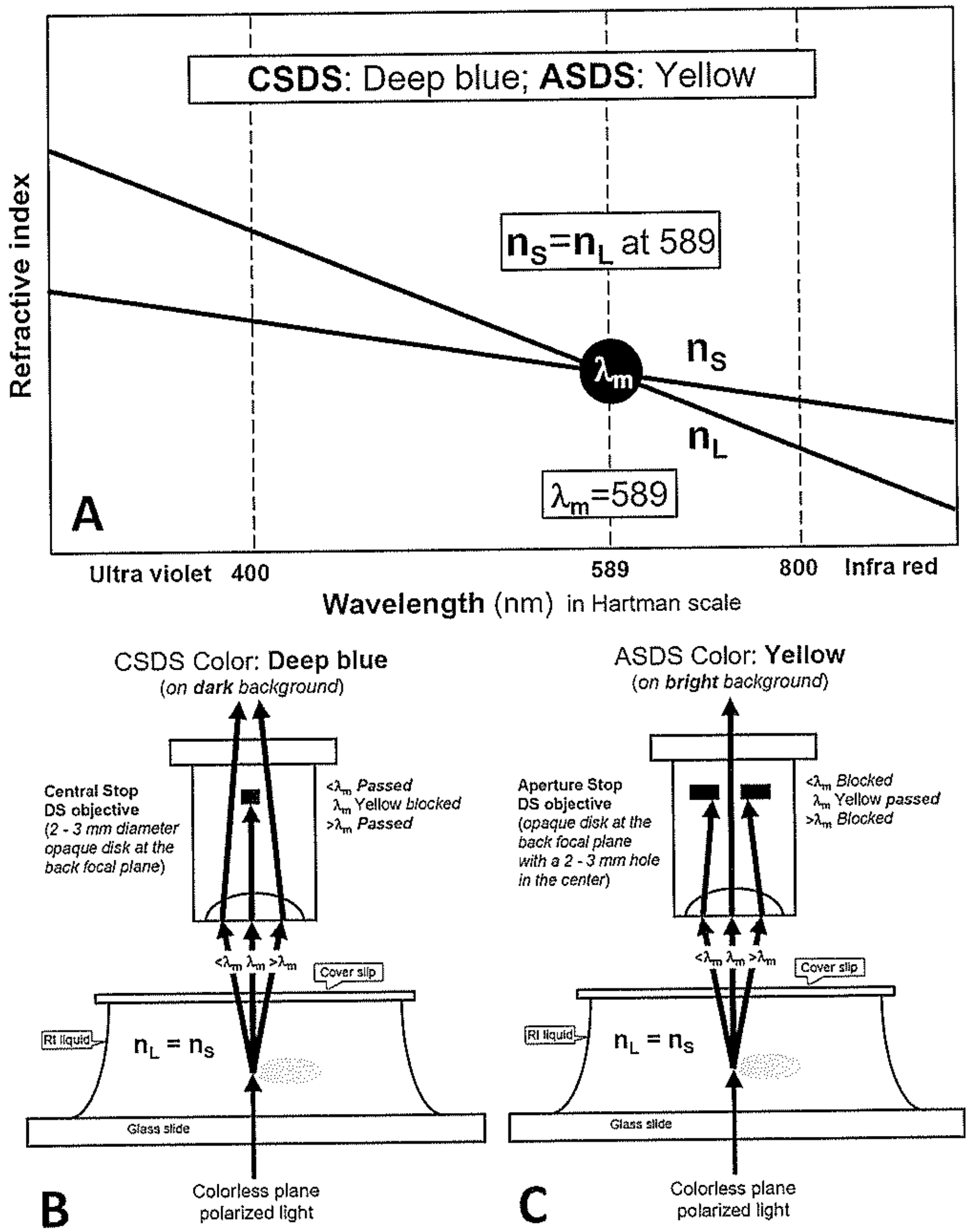

Figure 1. The principle of dispersion staining, showing the case of $n_S = n_L$ at 589.3 nm. A) The dispersion curves of solid and liquid intersect at 589.3 nm, λ_m = 589.3 nm; B) The central stop DS mode: λ_m is blocked by the CSDS objective lens; and C) The annular stop DS mode: λ_m is allowed to pass through the ASDS objective lens.

RI is the most important optical property of non-opaque minerals. It is therefore the primary diagnostic optical property used to identify asbestos minerals. Most environmental laboratories in the U.S. and Canada participate in the National Voluntary Laboratory Accreditation Program (NVLAP) administered by the National Institute of Standards and Technology (NIST), U.S. Department of Commerce. NVLAP requires the refractive indices α and γ of asbestos fibers to be determined by the immersion technique during routine bulk asbestos sample analysis. Generally, an attainable and reasonable accuracy is ≤0.005 for chrysotile, amosite, tremolite, actinolite, and anthophyllite, and ≤0.010 for crocidolite.

In many environmental laboratories, the high volume of samples demands that analysts minimize the amount of time spent on the determination of the required optical properties, particularly the refractive

indices. It is most desirable to determine both α and γ in a single preparation. There are three common techniques for assessing the sign and magnitude of the match/mismatch between a solid and its surrounding liquid: Becke line (3), dispersion staining (4, 5), and oblique illumination (6). Only the dispersion staining (DS) can meet the above specific needs for the routine PLM analysis of bulk asbestos samples in commercial environmental laboratories.

This paper proposes a rapid procedure for asbestos analysts to convert the observed DS color associated with α or γ for a specific asbestos mineral in a specific RI liquid through its matching wavelength λ_m into the corresponding numerical RI value with desirable accuracy.

DISPERSION STAINING TECHNIQUE

To fully understand dispersion staining, it is necessary to review the following basic concepts:

- Dispersive property: A physical property changing its value with optical wavelength. Refractive index is a dispersive property. The same material exhibits different RI values at different wavelengths.
- Refractive indices of the majority of materials decrease with increasing wavelength.
- Refractive indices of all asbestos minerals and RI liquids decrease with increasing wavelength.
- Hartmann equation (7): An equation relating refractive, n, with wavelength, λ:

$$n = a + b/\lambda + c^2/\lambda^2 + \ldots$$

where, a, b, and c are constants.

A 2-term Hartmann equation, $n = a + b/\lambda$ is sufficiently accurate to describe the quantitative relationship between n and λ for the purpose of discussion.

- Visible spectrum: 400–740 nm or 4,000–7,400 Å.
- Fraunhöfer spectral lines in the visible spectrum:

F (blue)	–486.1 nm	n_F	–RI at 486.1 nm
D (yellow)	–589.3 nm	n_D	–RI at 589.3 nm
C (red)	–656.3 nm	n_C	–RI at 656.3 nm

The F, D, and C wavelengths are rounded off in Figure 1A.

- The standard wavelength used to describe the RI of a material is D (yellow) or 589.3 nm. When we say a chrysotile fiber has $\gamma = 1.556$ and $\alpha = 1.548$, it is implied that the RI is for yellow light (D or 589.3 nm wavelength).
- Dispersion coefficient (DC), $[n_F - n_C]$, describes the dispersion power of a material. The larger the value, the higher the dispersion power. Generally, liquids have a higher DC than solids.
- Dispersion curve: Plot of RI n against wavelength λ, a nearly linear curve on a Hartmann dispersion chart ($n = a + b/\lambda$).
- Matching wavelength, λ_m: The wavelength at the intersection point of the dispersion curve of a solid with that of its surrounding liquid medium; the solid and liquid have the same RI at this wavelength.

Figure 2. The CSDS colors of NIST SRM (Standard Reference Material) 1866 chrysotile ($\alpha = 1.549$; $\gamma = 1.556$) in 1.550 HD-L RI liquid from DRIMMC at 23° C.

The immersion method is an effective way to determine the RI of small solid objects. An unknown non-opaque specimen is immersed in a series of liquid media with different RI values, and its RI is compared against that of the liquid. If a match in RI between the solid and liquid is reached, the unknown solid's RI (n_D^S) is considered to be equal to the liquid's RI (n_D^L).

Dispersion staining is a technique for the quantitative evaluation of the RI match/mismatch between n_D^S and n_D^L or the sign and magnitude of ($n_D^S - n_D^L$) using a special objective lens to filter out either the matching wavelength λ_m (central stop mode) or the complementary wavelengths of λ_m (annular stop mode). Figures 1B and 1C illustrate the principle of dispersion staining. The differences between the two DS modes are summarized in Table 1 (see Tables 1–16 on pages 61–69). Because the accuracy of the DS technique is dependent on the accuracy of assessing λ_m, the central stop dispersion staining (CSDS), which transmits the complementary wavelengths of λ_m on a dark background (Figure 2), is more accurate and suitable than the annular stop dispersion staining (ASDS) mode, which transmits λ_m on a bright background, for λ_m

assessment. Some types of dispersion staining objectives are equipped with a turning wheel or slider, which has both central and annular stops. One can quickly switch between the two modes of observation and combine both CSDS and ASDS colors to get a more accurate λ_m assessment.

THE RELATIONSHIP BETWEEN THE DISPERSION STAINING COLOR AND THE REFRACTIVE INDEX

Su (8–10) established the quantitative relationship among n, λ_m, $\Delta^L = [n_F - n_C]_{liquid}$, and $\Delta^S = [n_F - n_C]_{solid}$:

$$n_D{}^S = n_D{}^L + (\Delta^L - \Delta^S) \times k_D \qquad \textbf{Equation 1}$$

where

- $n_D{}^S$ – the RI value of the solid at 589.3 nm;
- $n_D{}^L$ – the RI of the liquid at 589.3 nm and t° C;
- Δ^L – the dispersion coefficient of the liquid, i.e., $[n_F - n_C]_{liquid}$;
- Δ^S – the dispersion coefficient of the solid, i.e., $[n_F - n_C]_{solid}$;
- k^D – a coefficient that is a function of λ_m and Fraunhöfer lines F, D, and C in accordance with the Hartmann dispersion relationship, which is equal to $[(\lambda_m - 200)^{-1} - (\lambda_D - 200)^{-1}] / [(\lambda_F - 200)^{-1} - (\lambda_C - 200)^{-1}]$ or $[(\lambda_m - 200)^{-1} - 0.002571] / 0.001304$.

1. The measurement of a solid's RI is replaced by the measurement of λ_m because both the liquid's RI and liquid's temperature are known. Dispersion staining is therefore a rapid and effective technique for assessing λ_m. That is why DS is ideally applicable for asbestos identification.
2. The solid's RI is the function of the dispersion coefficients of the solid and liquid, i.e., Δ^S and Δ^L. The Δ^S of asbestos minerals are always less than Δ^L of RI liquids.
3. For the purpose of building λ_m–t to asbestos RI conversion look-up tables, the equation is:

$$n_D{}^S = n_D{}^L + (\Delta^L - \Delta^S) \times k_D - (25 - t) \times dn/dt \qquad \textbf{Equation 2}$$

where t is the temperature of the RI liquid at measurement; dn/dt is the temperature coefficient of the liquid, a negative value.

THE HIGH DISPERSION RI LIQUIDS

The dispersion staining technique relies on the observed DS color to assess λ_m. A greater $(\Delta^L - \Delta^S)$ or greater dispersion coefficient of the RI liquid will produce more vibrant and better-defined DS colors, resulting in a more accurate λ_m.

There are two brands of high dispersion liquids on the market. Table 2 is a comparison of the dispersion coefficients of their high-dispersion series (HD for DRIMMC and E or B for Cargille) used in asbestos analysis.

On average, DRIMMC liquid's dispersion coefficient is 14.8% higher than that of Cargille liquids. For the most-frequently used 1.550 liquid, DRIMMC has two series HD-S and HD-L with almost identical dispersion coefficients. The author also found that the HD-S liquid maintains a pleasant aroma, whereas the HD-L has the pungent smell typical of conventional RI liquids.

THE DISPERSION COEFFICIENT OF ASBESTOS MINERALS

All asbestos minerals are crystalline materials and their dispersion coefficients are determined by their elemental composition and crystallographic structures. Despite the fact that the same type of asbestos minerals from different localities will have slight variations in chemistry and structure that may cause slight changes in the values of n_F, n_D, and n_C, their dispersion coefficients $[n_F - n_C]$ remain relatively stable or only slightly affected. Equation 1 indicates that if the dispersion coefficient of solid Δ^S is known, $n_D{}^S$ can be derived from the observed λ_m. Therefore, based on the dispersion coefficient data of six well-characterized asbestos minerals in Table 3, it is possible to establish quantitative relationships (Tables 4 and 5) between Δ^S and λ_m, which are equally applicable to the same type of asbestos from different locations.

PROCEDURE

1. Stereomicroscopical examination.

Examine the homogenized sample under a stereomicroscope. Based on the morphology and color, an initial identification can usually be reached for the type of asbestos present in the sample.

2. Check the alignment of the polarized light microscope.

Make sure that the microscope is properly aligned:

- DS objective and its central stop is centered;
- substage condenser is centered (if possible, set the microscope according to Köhler illumination principles); and
- the vibration (or privileged) directions of

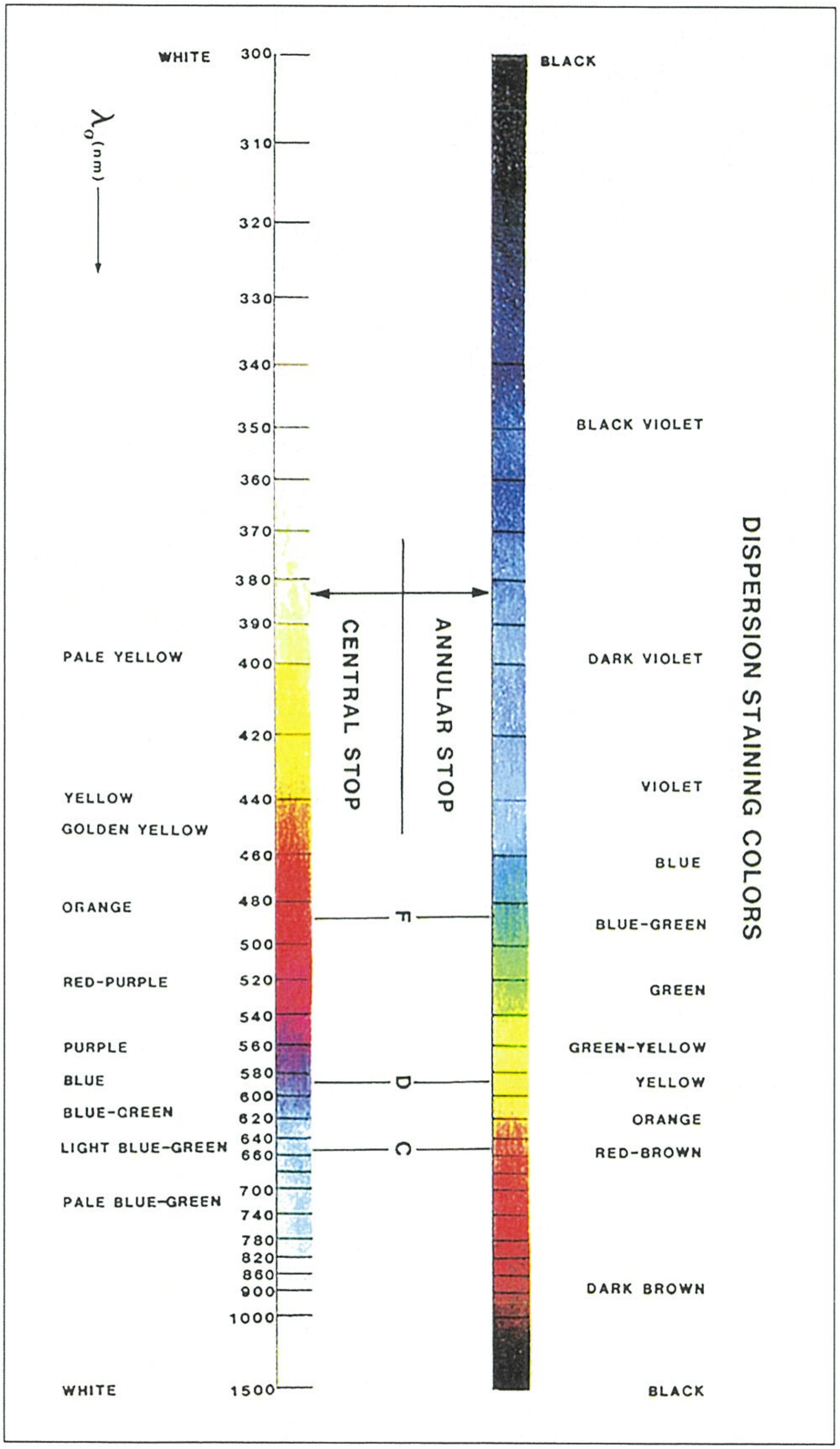

Figure 3. Converting dispersion staining color to corresponding λ_m, i.e., λ_0 in the chart (5).

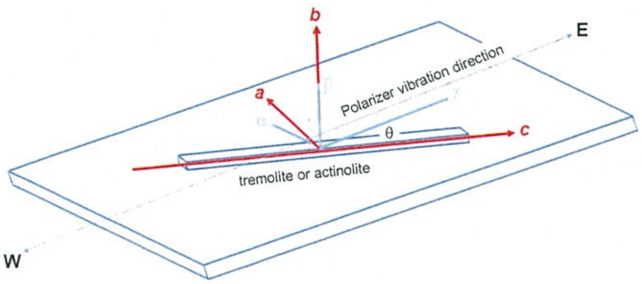

Figure 4. Optical orientation of tremolite and actinolite.

polarizer and analyzer are parallel to the E–W and N–S crosslines in the eyepiece, respectively.

3. Select a proper RI liquid to mount the sample.

Mount the suspected asbestos fibers in an appropriate RI liquid according to Table 6 DRIMMC liquid (13) or Table 7 Cargille liquid (14), which lists two cases: 1) for regulatory, legal, forensic, etc., which requires higher accuracy, and 2) for routine commercial analysis with less stringent accuracy requirements. For high-accuracy measurements such as regulatory, legal, and forensic analysis, etc., the rule of thumb is to choose RI liquids as close as possible to the RI's that will be measured. For example, there are chrysotile minerals whose RIs are significantly higher than those of the standard chrysotile from the NIST SRM 1866 set. In that case, 1.555 or 1.560, instead of 1.550, RI liquids should be used to determine γ (Table 6). When efficiency is a priority and the accuracy requirement is less stringent, choose an RI liquid higher than α and lower than γ so that the two RIs can be determined in a single preparation.

It is imperative to have a fresh surface of asbestos fibers in direct contact with the surrounding RI liquid. Sometimes, the surface of an asbestos bundle may be coated with matrix or binder materials. In this case, true DS colors may not be properly displayed. A simple and effective way to bring out the true DS colors is to grind or rub the fiber bundle with a steel needle or probe to break the fiber bundle into finer bundles to reveal some fresh surface in direct contact with the surrounding liquid.

4. Measure the temperature of the RI liquid.

Measure and record t (in °C) corresponding to the temperature of the RI liquid on the microscope slide. If the temperature of the liquid, slide, cover glass, and sample can be reasonably assumed to be in equilibrium with the room temperature, t can be assumed to be equal to the room temperature. The temperature data is needed for making a temperature correction. The light source of certain microscope might heat up the microscope stage and slide, resulting in an increase of 2° C or more in the liquid temperature.

5. Observe the central stop DS color associated with γ of the asbestos fibers.

Assuming the polarizer's linear vibration direction is E–W, refer to Table 8 to orient the asbestos fiber for measurement. It is simple to locate both α and γ for chrysotile, amosite, and crocidolite, all of which exhibit "uniaxial" characteristics, by following the description in Table 8. A small range of DS colors is usually displayed. Record the prevalent CSDS color (Figure 3) as the measure of λ_m of α.

It is not easy, however, to locate α and γ for tremolite and actinolite, both of which exhibit monoclinic extinction characteristics. Their fibrous morphology makes it even harder to do so because it is impossible to obtain the interference figure of a fine fiber or fiber bundle to locate α or γ. The only measurable property related to the γ location is the extinction angle θ. For tremolite and actinolite, γ and α are in the a–c crystallographic plane, i.e., the plane containing both a- and c-axes, or (010) plane, in which γ exhibits a maximum extinction angle to the c-axis, the fiber elongation axis (Figure 4).

By definition, the extinction angle is defined as the acute angle between γ and the fiber elongation axis (c-axis for tremolite and actinolite). Because thin fibers in a RI liquid can rotate freely around their elongation axes, a randomly chosen tremolite or actinolite fiber may not exhibit its true extinction angle but a range of extinction angles from 0° (parallel extinction) up to its true extinction angle, which may be 20° or more; it is mostly between 15° and 18° (15) Rotate a tremolite or actinolite fiber to the extinction position near the E–W crossline (with an E–W polarizer) and measure its extinction angle relative to the E–W crossline. After measuring at least a dozen or more oblique extinction fibers, the one that exhibits the largest extinction angle is the fiber having a RI statistically closest to the true γ. Record its CSDS color as a measurement of the true γ. Once γ is found, one can rotate the fiber 90° and α is now parallel to the E–W polarizer. The CSDS color of α can now be recorded.

It is not always possible to locate the true γ because the fiber with the largest extinction angle statistically may not be the true γ but a γ' close to γ. It will be necessary to evaluate the possible deviation of a γ' from γ if the apparent (observed) extinction angle is less than the true extinction angle. Figure 5

is the α–γ section of the optical indicatrix of tremolite or actinolite, which contains the c-axis. θ is the true extinction angle. The γ' values for any direction between γ and c can be easily calculated. Table 9 is the calculation of the possible RI (γ') values and their deviations from the true γ value (γ–γ') for a randomly-chosen oblique extinction fiber when the fiber has an extinction angle of 20°. According to Table 9, any oblique extinction fiber's γ' will not deviate from the true γ by more than 0.0035, well within the acceptable absolute error of 0.005 or higher required by NVLAP in its biannual proficiency testing. Therefore, it can be concluded that, as long as an oblique extinction fiber with a distinctive extinction angle is measured, its γ' value will meet the NVLAP accuracy requirements for γ; the same conclusion is true for α.

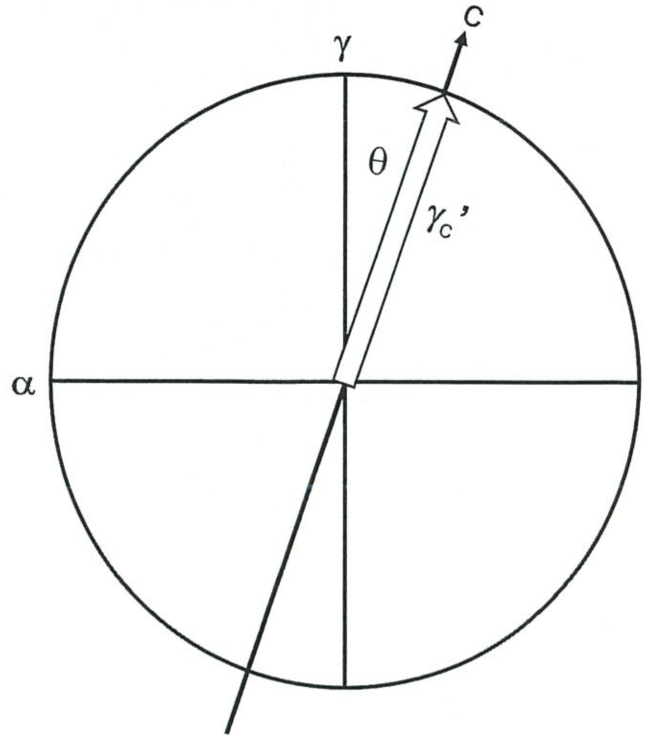

Figure 5. In this α–γ section of the optical indicatrix of tremolite and actinolite, the RI value of a direction is equal to the corresponding radius of the ellipse, e.g., the RI along the c-axis or the fiber elongation axis is the radius γ_c'. The extinction angle is θ, i.e., the angle between γ and c. Any fiber that exhibits an apparent (observed) extinction angle less than θ will have an RI (γ') equivalent to its corresponding radius between γ and γ_c' (Table 9).

6. Convert the observed DS color into the corresponding matching wavelength λ_m between the asbestos fiber and the RI liquid used by referring to Table 10 and Figure 3.

Unlike Figure 3, the increments of the matching wavelength in Table 10 are not a uniform 20 nm (for the most part). The increments in Table 10 are coarser than those of Figure 3. For example, if an observed CSDS color is yellow-orange, which does not fall right on a specific color but between two adjacent colors: golden yellow (455 nm) and orange (485 nm). The color can be interpolated as 470 nm. For an experienced analyst, one can assign the color to be 460 nm if closer to golden yellow or 480 nm if closer to orange.

7. Find out the numerical value of γ corresponding to the observed λ_m and t.

Search the conversion look-up table, e.g., Table 4 (DRIMMC liquid) or Table 5 (Cargille liquid) for chrysotile, or the attached conversion tables for other asbestos minerals (listed in Table 11 and downloadable by scanning the QR code on page 51) to convert the observed λ_m and t into the corresponding numerical value of the RI γ.

Dispersion staining does not require that the RI of the liquid match the solid's RI at exactly 589.3 nm, i.e., $n_D^S = n_D^L$; n_D^L could be lower or higher than n_D^S as long as λ_m is within the visible range 400 to 740 nm. DS exhibits (n_D^S–n_D^L) as a DS color, which is a function of (n_D^S– n_D^L). In other words, the DS color tells us whether n_D^S is lower or higher than n_D^L and by how much (Equation 1). Because n_D^L is known, n_D^S is then determined. All required computations by Equation 1 are built into the look-up Table 4 (DRIMMC liquids) or Table 5 (Cargille liquids) to facilitate the quick solution of n_D^S.

8. Observe the DS color associated with α of the asbestos fibers.

For chrysotile, amosite, and crocidolite, rotate the fiber 90° from the γ position to measure α. Again, a range of DS colors is usually displayed. Record the prevalent CSDS color (e.g., Figure 2 for chrysotile) as the measure of α.

For tremolite or actinolite, as mentioned in procedure No. 5, the direction 90° from γ is α. For anthophyllite, trial and error is still the only viable approach to finding α. Align the fiber parallel to the N–S crossline with an E–W polarizer. At this position, the RI displayed could be any value between α and β, most likely α'. Measure at least a dozen fibers, and the longest matching wavelength color (Table 10 and Figure 3), i.e., corresponding to the lowest RI value, is the closest to α.

9. Convert the observed DS color into the corresponding matching wavelength λ_m between the asbestos

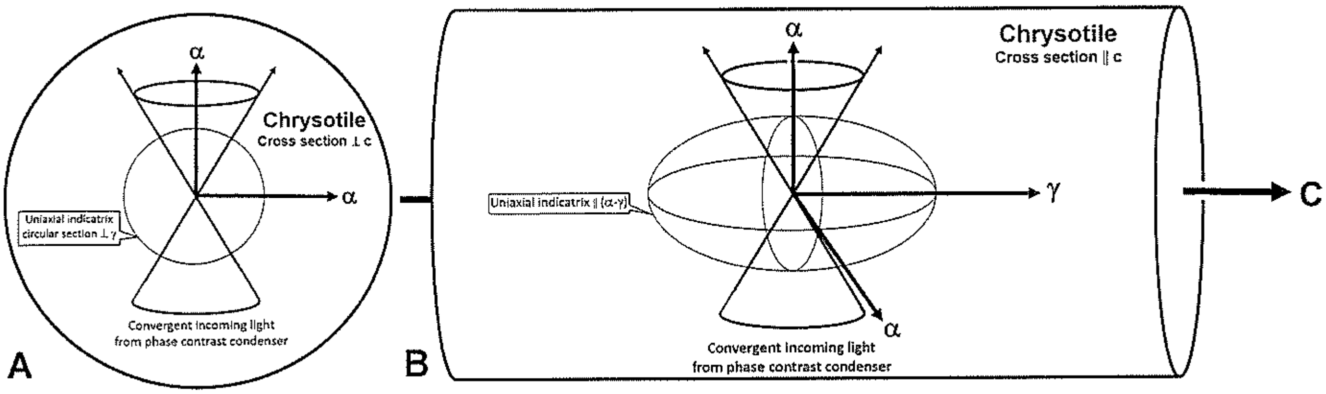

Figure 6. Cross sections of the indicatrix of chrysotile: A) ⊥ γ and B) || (α–γ).

fiber and the RI liquid used by referring to Table 10 and Figure 3.

Although both Table 10 and Figure 3 are capable of converting DS colors into the corresponding λ_m, Table 10 is preferred because the colors of Figure 3 are affected by quite a few factors, such as the color temperature of the microscope light source, intensity of the incident light, printer's color fidelity, etc.

10. Find out the numerical value of α corresponding to the observed λ_m and t.

Search the conversion table, e.g., Table 4 (DRIMMC liquid) or Table 5 (Cargille liquid) for chrysotile, or conversion tables for other asbestos minerals (listed in Table 11 and downloadable by scanning the QR code on page 51) to convert the observed λ_m and t into the corresponding numerical value of RI γ.

HIGH-MAGNIFICATION DISPERSION STAINING OBJECTIVE AND PHASE CONTRAST DISPERSION STAINING

The best result for the DS technique is obtained using a 10× objective lens because its small (0.17–0.25) numerical aperture (NA) is best suited to achieve an axial light beam. The paramount importance of using an axial light beam in RI measurement cannot be overemphasized. However, sometimes the specimen particle is so minute, higher magnification objectives are desirable. To meet this demand primarily in asbestos analysis, a microscope manufacturer introduced a 40× DS objective lens with an NA = 0.75 (16), which generates a 97° light cone to illuminate the whole field of view. This light cone contains a wave normal whose angle to the plane of the slide ranges from 0° to 42°. For isotropic crystals, its optical indicatrix (7, 17) is a sphere, meaning every direction exhibits the same RI. The circular cross section of the uniaxial optical indicatrix perpendicular is similar to the c crystallographic axis. Mineralogically speaking, chrysotile is a monoclinic crystal and biaxial. Because of the strain-related deformation in the crystal structure, the asbestiform chrysotile forms a tabular fibril that is composed of concentrically or spirally curved layers (18). It behaves optically like a uniaxial crystal with two principal refractive indices, ω (equivalent to α) and ε (equivalent to γ), with a singular circular section perpendicular to γ, i.e., the c-axis (Figure 6A). Only in the case of an isotropic crystal or the circular section of a uniaxial crystal, is a conical convergent beam capable of measuring the target RI, i.e., n for isotropic and ω (α) for uniaxial. It is acceptable for an analyst to use a 40× DS objective to measure α of chrysotile. It is not acceptable, however, to use the same objective to measure γ of chrysotile because the wave normal is up to ≈42° in the conical convergent beam, and so it is not parallel to the γ direction. The RI measured by the range of the wave normal is γ' instead of the true γ (Figure 6B).

Therefore, the 40× DS objective is capable of measuring α of chrysotile but not the true γ. From a mineralogy standpoint, it is incapable of measuring α and γ of the five amphibole asbestos minerals because their crystallographic systems are either monoclinic or orthorhombic. For monoclinic and orthorhombic asbestos minerals, the 40× DS objective can only measure α' and γ' instead of true α and true γ.

Yet for practical reasons, it must be pointed out that in the case of fibers exhibiting low birefringence recording γ' may be within the NVLAP-acceptable error for γ (see the error estimate in Table 9). And it is acceptable to use the 40× DS objective for RI measurement of asbestos minerals even though one is not measuring the true α or γ but an α' reasonably close to the true α and a γ' reasonably close to the true γ.

The above analysis is equally applicable to phase contrast DS, whose light path is illustrated in Figure 7. The highly convergent incoming light beams will result in a highly convergent wave normal cone, which can only measure chrysotile's α but not γ. Nor can it measure the true α and γ of any biaxial crystals, such as the five amphibole asbestoses.

Again, for practical reasons, in the case of fibers exhibiting low birefringence recording γ' may be within the NVLAP-acceptable error for γ (see the error estimate in Table 9). And it is acceptable to use phase contrast dispersion staining for RI measurement of asbestos minerals even though one is not measuring the true α or γ but an α' reasonably close to the true α and a γ' reasonably close to the true γ.

CALIBRATION OF RI LIQUIDS USING CARGILLE OPTICAL GLASS STANDARDS

To ensure the accuracy of measurement, it is necessary to make sure that the RI liquids used have correct RI values. The calibration of RI liquids can only be accurately performed using an Abbe refractometer. When an Abbe refractometer is not available, an alternative means of calibration (in fact it is not a calibration in its strict sense but practically a verification) is by using optical glasses that have accurate and precise RI values, such as the optical glass standards manufactured by Cargille (20). Since the NVLAP program uses "calibration" in its documents and allows the use of optical glass standards, we can follow NVLAP program usage, yet it is actually a "verification" of whether an RI liquid is within ±0.004 of its $n_D^{25°}$ C value. There are three Cargille Reference Sets on the market: M-7, M-24, and M-25 (14). Table 12 summarizes the parameters of Cargille glasses suitable for RI liquid calibration. There are many overlaps among the three sets with the same or different lot numbers.

The procedure for the calibration of RI liquids using optical glass standards is similar to the above procedure for the measurement of RI of asbestos minerals using RI liquids. In asbestos identification, a liquid with known RI is the "known," and the asbestos mineral's RI is the "unknown" to be measured. In the RI liquid calibration, the role is reversed: the optical glass standard with known RI is the "known," and the RI of the liquid is the "unknown" to be measured. Therefore, their operational procedures are the same. However, the equation used in generating the look-up conversion tables is different in terms of the sign of the temperature correction.

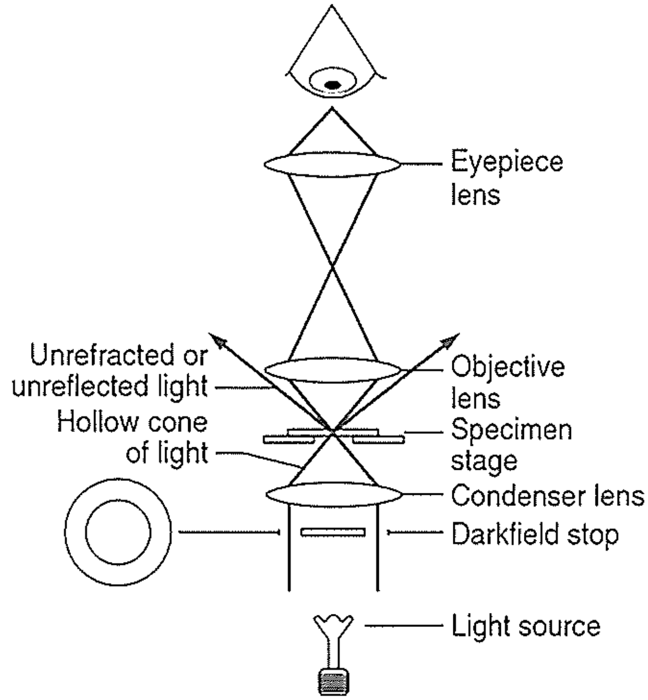

Figure 7. The light path of phase contrast microscope (19).

$$n_D^S = n_D^L + (DL-DS) \times k_D + (25-T) \times dn/dt \quad \textbf{Equation 3}$$

After finding the matching wavelength λ_m at temperature t, the RI of liquid at D wavelength (589.3 nm) and 25° C can be read from the look-up conversion tables in Table 13 (DRIMMC liquid) or Table 14 (Cargille liquid), which are built using Equation 3 for the liquid-glass combinations in Table 15. Table 16 is a recommended form for recording RI liquid calibration results using Cargille glass standards.

SUMMARY

1. Dispersion staining is an effective technique for quantifying the RI difference between a non-opaque solid and its surrounding RI liquid medium. Between the two modes of DS, central stop dispersion staining is the most suitable for routine analysis in bulk asbestos identification.

2. In the majority of cases, one bulk sample preparation is sufficient to measure both α and γ to the desired accuracy required by NVLAP. For NVLAP proficiency testing, separate RI liquids for α and γ are recommended (Tables 6 and 7).

3. A full suite of 40 conversion look-up tables has been developed to facilitate the conversion of the observed matching wavelength λ_m, and temperature t,

to the corresponding refractive index value for the six regulated asbestos minerals. Those tables can be downloaded by scanning the QR code on page 51.

4. The RI liquids from DRIMMC have relatively higher dispersion coefficients than other RI liquids and are capable of producing more vibrant and better-defined dispersion staining colors leading to better accuracy in the assessment of the matching wavelength λ_m. The author also found that the HD-S 1.550 liquid maintains a pleasant aroma, without the pungent smell typical of conventional RI liquids.

5. Despite the fact that the high-magnification DS objective lens is only adequate to measure chrysotile's α but not its γ, or the α or γ of the five amphiboles, it is practically capable of obtaining an α' reasonably close to the true α in the case of amphiboles and a γ' reasonably close to the true γ in the case of chrysotile and amphiboles. The same is true for the high-magnification phase contrast objective lens.

6. In the absence of an Abbe refractometer, RI liquids can be calibrated (verified) using optical glass standards. Twenty-two comprehensive conversion look-up tables for both DRIMMC and Cargille RI liquids have been constructed and can be downloaded by scanning the QR code on page 51.

ACKNOWLEDGMENTS

I would like to thank Peter M. Cooke, MICA (Microscopy Instruction, Consultation and Analysis), for his critical reviews, inspirational comments, and constructive contributions to the improvement of this paper. Valuable advice from Dr. Mickey E. Gunter, Emeritus University Distinguished Professor at University of Idaho, is greatly appreciated. I also thank both Cargille Laboratories and Delaware Research Institute of Microscopy and Material Characterization LLC for kindly providing the specifications of their products.

REFERENCES CITED

1. U.S.C. Asbestos Hazard Emergency Response Act. Title 15 — Commerce and Trade, Chapter 53 — Toxic Substances Control, Subchapter II, 1986.

2. U.S. EPA. 40 CFR Appendix E to Subpart E of Part 763 — Interim Method of the Determination of Asbestos in Bulk Insulation Samples, 1982.

3. Bloss, F.D. An *Introduction to the Methods of Optical Crystallography*, First Edition, Holt, Rinehart & Winston, Inc.: New York, vii + 294 pp, 1961.

4. Wilcox, R. "Refractive Index Determination Using the Central Focal Masking Technique with Dispersion Colors," *American Mineralogist*, 68, pp 1226–1236, 1983.

5. McCrone, W.C. *Asbestos Identification*, McCrone Research Institute: Chicago, 1987.

6. Stoiber, R.E. and Morse, S.A. *Crystal Identification with the Polarized Light Microscope*, Chapman & Hall: New York, 1994.

7. Bloss, F.D. *Optical Crystallography*, Mineralogical Society of America: Washington, D.C., 231 pp, 1999.

8. Su, S.C. "Determination of Refractive Index of Solids by Dispersion Staining Method — An Analytical Approach," C.L. Rieder, ed., Proceedings of 51st Annual Meeting of the Microscopy Society of America, pp 456–457, 1993.

9. Su, S.C. "Dispersion Staining: Principles, Analytical Relationships and Practical Applications to the Determination of Refractive Index," *The Microscope*, 46, pp 123–146, 1998.

10. Su, S.C. "A Rapid and Accurate Procedure for the Determination of Refractive Indices of Asbestos Minerals," *American Mineralogist*, 88, pp 1979–1982, 2003.

11. NIST SRM. *Certificate of Analysis: Standard Reference Material 1866*, National Institute of Standard and Technology: Gaithersburg, MD, 1988A.

12. NIST SRM. *Certificate of Analysis: Standard Reference Material 1867*, National Institute of Standard and Technology: Gaithersburg, MD, 1988B.

13. DRIMMC. *Specifications of High Dispersion Refractive Index Liquids*, Delaware Research Institute of Microscopy and Material Characterization: Newark, DE, 2021.

14. Cargille M-24 Reference Set Precise Optical Values. RS-M24-T-0172, Cargille Laboratories: Cedar Grove, NJ, 2017.

15. Verkouteren, J.R. and Wylie, A.G. "The Tremolite–Actinolite–Ferro-Actinolite Series: Systematic Relationships Among Cell Parameters, Composition, Optical Properties, and Habit, and Evidence of Discontinuities," *American Mineralogist*, 85, pp 1239–1254, 2000.

16. Meiji Techno MA938D Dispersion Staining Plan for Transmitted Light 40× Objective Polarizing Brightfield Objective for MT9000, MT9400, MT9500 and MT9900 Polarizing Upright Series, https://meijitechno.com/ma938d-transmitted-light-40x-objective (accessed July 26, 2022).

17. Dyar, M.D. and Gunter, M.E. *Mineralogy and Optical Mineralogy*, 2nd Edition, Mineralogical Society of America: Chantilly, VA, 708 pp, 2019.

18. Yada, K. "Study of Microstructure of Chrysotile Asbestos by High-Resolution Electron Microscopy," *Acta Crystallographica*, A27, pp 659–664, 1971.

19. TheFreeDictionary.com by Farlex, Inc. "Phase-contrast microscope," https://medical-dictionary.thefreedictionary.com/phase-contrast+microscope (accessed July 26, 2022).

20. Su, S.C. "Calibration of Refractive Index Liquids Using Optical Glass Standards with Dispersion Staining Technique," *The Microscope*, 40, pp 95–108, 1992. ■

See Tables 1–16 on pages 61–69

Table 1. Comparison of the Two Modes of Dispersion Staining Techniques

Mode of dispersion staining		Central Stop	Annular Stop
Objective lens used		Central stop	Annular stop
Wavelengths observed		($<\lambda_m$) + ($>\lambda_m$)	λ_m
DS color observed at different n_S vs. n_L relationship	$n_S >> n_L$	Ver pale yellow	Black violet
	$n_S > n_L$	Yellowish-reddish	Bluish-greenish
	$n_S = n_L$	Deep blue	Yellow
	$n_S < n_L$	Bluish-greenish	Orangish-brownish
	$n_S << n_L$	Very pale blue-green	Black brown
Background		Darkfield	Brightfield
Accuracy of assessing λ_m		Higher	Lower

Table 2. Dispersion Coefficients of DRIMMC and Cargille RI Liquids

RI Liquid	1.550	1.605	1.610	1.615	1.620	1.625	1.630	1.635	1.640	1.680	1.700
DRIMMC[1]	HD-S	HD-L	HD-L	HD-L	HD-L	HD-L	HD-L	HD-L	HD-L	HD-L	HD-L
	0.0274	0.0313	0.0315	0.0319	0.0323	0.0327	0.0328	0.0332	0.0338	0.0383	0.0378
Cargille[2]	E	E	E	E	E	E	E	E	E	B	B
	0.0267	0.0243	0.0251	0.0259	0.0275	0.0275	0.0283	0.0291	0.0299	0.0348	0.0370

[1]Manufactured by Delaware Research Institute of Microscopy and Material Characterization LLC.
[2]Manufactured by Cargille Laboratory.

Table 3. Refractive Indices and Dispersion Coefficients [n_F–n_C] of Six Asbestos Minerals

Asbestos	RI	n_F	n_D	n_C	[n_F–n_C]	Reference
Chrysotile	α	1.5563	1.5486	1.5455	0.0107*	NIST SRM 1866 (11)
	γ	1.5649	1.5564	1.5531	0.0119*	
Grunerite (Amosite)	α	1.6937	1.6790	1.6731	0.0206	
	γ	1.7157*	1.7010	1.6951	0.0206*	
Riebeckite (Crocidolite)	α	1.7132	1.7015	1.6971	0.0161	Figures 104A, 104B (5)
	γ	1.7206	1.7072	1.7032	0.0174	
Tremolite	α	1.6128	1.6063	1.6036	0.0092	NIST SRM 1867 (12)
	β	1.6299	1.6230	1.6201	0.0098	
	γ	1.6423	1.6343	1.6310	0.0113	
Actinolite	α	1.6201	1.6126	1.6095	0.0106	
	β	1.6369	1.6288	1.6254	0.0115	
	γ	1.6485	1.6393	1.6355	0.0130	
Anthophyllite	α	1.6227	1.6148	1.6116	0.0111	
	β	1.6350	1.6273	1.6241	0.0109	
	γ	1.6449	1.6362	1.6326	0.0123	

*Recalculated from the regression analysis of SRM 1866 original data.

Table 4. λ_m and t to RI Conversion for Chrysotile in DRIMMC 1.550 (HD-S or L)

λ_m (nm)	α							γ						
	17° C	19° C	21° C	23° C	25° C	27° C	29° C	17° C	19° C	21° C	23° C	25° C	27° C	29° C
300	1.648	1.647	1.646	1.645	1.644	1.643	1.642	1.641	1.640	1.639	1.638	1.637	1.636	1.635
320	1.627	1.626	1.625	1.624	1.623	1.622	1.621	1.622	1.621	1.620	1.619	1.618	1.617	1.616
340	1.612	1.611	1.610	1.609	1.608	1.607	1.606	1.608	1.607	1.606	1.605	1.604	1.603	1.602
360	1.601	1.600	1.599	1.598	1.597	1.596	1.595	1.597	1.596	1.595	1.594	1.593	1.592	1.591
380	1.592	1.591	1.590	1.589	1.588	1.587	1.586	1.589	1.588	1.587	1.586	1.585	1.584	1.583
400	1.585	1.584	1.583	1.582	1.581	1.580	1.579	1.582	1.581	1.580	1.579	1.578	1.578	1.577
420	1.579	1.578	1.577	1.576	1.575	1.574	1.573	1.577	1.576	1.575	1.574	1.573	1.572	1.571
440	1.574	1.573	1.572	1.571	1.570	1.569	1.568	1.573	1.572	1.571	1.570	1.569	1.568	1.567
460	1.570	1.569	1.568	1.567	1.566	1.565	1.564	1.569	1.568	1.567	1.566	1.565	1.564	1.563
480	1.567	1.566	1.565	1.564	1.563	1.562	1.561	1.566	1.565	1.564	1.563	1.562	1.561	1.560
500	1.564	1.563	1.562	1.561	1.560	1.559	1.558	1.563	1.562	1.561	1.560	1.559	1.558	1.557
520	1.561	1.560	1.559	1.558	1.557	1.556	1.555	1.560	1.559	1.558	1.557	1.557	1.556	1.555
540	1.559	1.558	1.557	1.556	1.555	1.554	1.553	1.558	1.557	1.556	1.555	1.554	1.553	1.552
560	1.557	1.556	1.555	1.554	1.553	1.552	1.551	1.556	1.555	1.554	1.553	1.552	1.551	1.550
580	1.555	1.554	1.553	1.552	1.551	1.550	1.549	1.555	1.554	1.553	1.552	1.551	1.550	1.549
600	1.553	1.552	1.551	1.550	1.549	1.548	1.547	1.553	1.552	1.551	1.550	1.549	1.548	1.547
620	1.552	1.551	1.550	1.549	1.548	1.547	1.546	1.552	1.551	1.550	1.549	1.548	1.547	1.546
640	1.550	1.549	1.548	1.547	1.546	1.545	1.544	1.550	1.549	1.548	1.547	1.547	1.546	1.545
660	1.549	1.548	1.547	1.546	1.545	1.544	1.543	1.549	1.548	1.547	1.546	1.545	1.544	1.543
680	1.548	1.547	1.546	1.545	1.544	1.543	1.542	1.548	1.547	1.546	1.545	1.544	1.543	1.542
700	1.547	1.546	1.545	1.544	1.543	1.542	1.541	1.547	1.546	1.545	1.544	1.543	1.542	1.541
720	1.546	1.545	1.544	1.543	1.542	1.541	1.540	1.546	1.545	1.544	1.543	1.542	1.541	1.540
740	1.545	1.544	1.543	1.542	1.541	1.540	1.539	1.546	1.545	1.544	1.543	1.542	1.541	1.540
760	1.544	1.543	1.542	1.541	1.540	1.539	1.538	1.545	1.544	1.543	1.542	1.541	1.540	1.539
780	1.543	1.542	1.541	1.540	1.539	1.538	1.537	1.544	1.543	1.542	1.541	1.540	1.539	1.538
800	1.543	1.542	1.541	1.540	1.539	1.538	1.537	1.543	1.542	1.541	1.540	1.539	1.538	1.537
850	1.541	1.540	1.539	1.538	1.537	1.536	1.535	1.542	1.541	1.540	1.539	1.538	1.537	1.536
900	1.539	1.539	1.538	1.537	1.536	1.535	1.534	1.541	1.540	1.539	1.538	1.537	1.536	1.535
950	1.538	1.537	1.536	1.535	1.534	1.533	1.532	1.539	1.538	1.537	1.536	1.535	1.534	1.534
1000	1.537	1.536	1.535	1.534	1.533	1.532	1.531	1.538	1.537	1.536	1.535	1.535	1.534	1.533

Table 5. λ_m and t to RI Conversion for Chrysotile in Cargille 1.550 (E)

λ_m	α							γ						
(nm)	17° C	19° C	21° C	23° C	17° C	19° C	21° C	17° C	19° C	21° C	23° C	17° C	19° C	21° C
300	1.645	1.644	1.643	1.642	1.641	1.640	1.639	1.638	1.637	1.636	1.635	1.634	1.633	1.632
320	1.625	1.624	1.623	1.622	1.621	1.620	1.619	1.619	1.618	1.617	1.616	1.615	1.614	1.613
340	1.610	1.609	1.608	1.607	1.606	1.605	1.604	1.606	1.605	1.604	1.603	1.602	1.601	1.600
360	1.599	1.598	1.597	1.596	1.595	1.594	1.593	1.596	1.595	1.594	1.593	1.592	1.591	1.590
380	1.591	1.590	1.589	1.588	1.587	1.586	1.585	1.588	1.587	1.586	1.585	1.584	1.583	1.582
400	1.584	1.583	1.582	1.581	1.580	1.579	1.578	1.581	1.581	1.580	1.579	1.578	1.577	1.576
420	1.578	1.577	1.576	1.575	1.574	1.573	1.572	1.576	1.575	1.574	1.573	1.572	1.571	1.570
440	1.573	1.573	1.572	1.571	1.570	1.569	1.568	1.572	1.571	1.570	1.569	1.568	1.567	1.566
460	1.570	1.569	1.568	1.567	1.566	1.565	1.564	1.568	1.567	1.566	1.565	1.564	1.563	1.563
480	1.566	1.565	1.564	1.563	1.562	1.561	1.560	1.565	1.564	1.563	1.562	1.561	1.560	1.559
500	1.563	1.562	1.561	1.560	1.559	1.558	1.557	1.563	1.562	1.561	1.560	1.559	1.558	1.557
520	1.561	1.560	1.559	1.558	1.557	1.556	1.555	1.560	1.559	1.558	1.557	1.556	1.555	1.554
540	1.558	1.557	1.557	1.556	1.555	1.554	1.553	1.558	1.557	1.556	1.555	1.554	1.553	1.552
560	1.556	1.555	1.554	1.554	1.553	1.552	1.551	1.556	1.555	1.554	1.553	1.552	1.551	1.550
580	1.555	1.554	1.553	1.552	1.551	1.550	1.549	1.555	1.554	1.553	1.552	1.551	1.550	1.549
600	1.553	1.552	1.551	1.550	1.549	1.548	1.547	1.553	1.552	1.551	1.550	1.549	1.548	1.547
620	1.552	1.551	1.550	1.549	1.548	1.547	1.546	1.552	1.551	1.550	1.549	1.548	1.547	1.546
640	1.550	1.549	1.548	1.547	1.546	1.545	1.544	1.551	1.550	1.549	1.548	1.547	1.546	1.545
660	1.549	1.548	1.547	1.546	1.545	1.544	1.543	1.549	1.548	1.547	1.546	1.545	1.545	1.544
680	1.548	1.547	1.546	1.545	1.544	1.543	1.542	1.548	1.547	1.546	1.545	1.544	1.543	1.543
700	1.547	1.546	1.545	1.544	1.543	1.542	1.541	1.547	1.546	1.545	1.544	1.544	1.543	1.542
720	1.546	1.545	1.544	1.543	1.542	1.541	1.540	1.547	1.546	1.545	1.544	1.543	1.542	1.541
740	1.545	1.544	1.543	1.542	1.541	1.540	1.539	1.546	1.545	1.544	1.543	1.542	1.541	1.540
760	1.544	1.543	1.542	1.541	1.540	1.539	1.538	1.545	1.544	1.543	1.542	1.541	1.540	1.539
780	1.544	1.543	1.542	1.541	1.540	1.539	1.538	1.544	1.543	1.542	1.541	1.540	1.539	1.538
800	1.543	1.542	1.541	1.540	1.539	1.538	1.537	1.544	1.543	1.542	1.541	1.540	1.539	1.538
850	1.541	1.540	1.539	1.538	1.537	1.536	1.535	1.542	1.541	1.540	1.539	1.538	1.537	1.536
900	1.540	1.539	1.538	1.537	1.536	1.535	1.534	1.541	1.540	1.539	1.538	1.537	1.536	1.535
950	1.539	1.538	1.537	1.536	1.535	1.534	1.533	1.540	1.539	1.538	1.537	1.536	1.535	1.534
1000	1.538	1.537	1.536	1.535	1.534	1.533	1.532	1.539	1.538	1.537	1.536	1.535	1.534	1.533

1.545

Table 6. Selection of DRIMMC Immersion Liquids for Asbestos Analysis

Asbestos	RI	High Accuracy Required (regulatory, litigation, forensic, etc.)	Routine Samples
Chrysotile	α	1.546 / 1.550 (HD or HD-L)*	1.550 (HD-S or L)
	γ	1.550 / 1.560 (HD or HD-L)*	
Grunerite (Amosite)	α	1.680 (HD or HD-L)	1.680 (HD or HD-L)
	γ	1.700 (HD or HD-L)	
Riebeckite (Crocidolite)	α	1.700 (HD or HD-L)	1.680 (HD or HD-L)
	γ	1.680 (HD or HD-L)	
Tremolite	α	1.605 / 1.610 / 1.615 (HD or HD-L)	1.620 (HD or HD-L) or 1.625 (HD or HD-L)
	γ	1.630 / 1.635 (HD or HD-L)	
Actinolite	α	1.605 / 1.610 / 1.615 (HD or HD-L)	
	γ	1.635 / 1.640 (HD or HD-L)	
Anthophyllite	α	1.605 / 1.610 / 1.615 (HD or HD-L)	
	γ	1.630 / 1.635 / 1.640 (HD or HD-L)	

*There are chrysotile minerals whose refractive indices are higher than those of the NIST SRM 1866 chrysotile.

Table 7. Selection of Cargille RI Liquids for Asbestos Analysis

Asbestos	RI	High Accuracy Required (regulatory, litigation, forensic, etc.)	Routine Samples
Chrysotile	α	1.546 / 1.550 (E)*	1.550 (E)
	γ	1.550 / 1.560 (E)*	
Grunerite (Amosite)	α	1.680 (B)	1.680 (E)
	γ	1.700 (B)	
Riebeckite (Crocidolite)	α	1.700 (B)	1.680 (E)
	γ	1.680 (B)	
Tremolite	α	1.605 / 1.610 / 1.615 (E)	1.620 (E) or 1.625 (E)
	γ	1.630 / 1.635 (E)	
Actinolite	α	1.605 / 1.610 / 1.615 (E)	
	γ	1.635 / 1.640 (E)	
Anthophyllite	α	1.605 / 1.610 / 1.615 (E)	
	γ	1.630 / 1.635 / 1.640 (E)	

*There are chrysotile minerals whose refractive indices are higher than those of the NIST SRM 1866 chrysotile.

Table 8. Fiber Orientation for Measuring α and γ (Assuming an E–W Polarizer)

Asbestos	Fiber Orientation α	Fiber Orientation γ	Remarks
Chrysotile	N–S	E–W	—
Amosite	N–S	E–W	—
Crocidolite	E–W	N–S	The only negative sign of elongation asbestos.
Tremolite	Nearly N–S	Nearly E–W	Maximum extinction angle for γ; 90° from γ is α.
Actinolite	Nearly N–S	Nearly E–W	Maximum extinction angle for γ; 90° from γ is α.
Anthophyllite	N–S	E–W	E–W is γ; longest λ_m in N–S is α.

Table 9. Relationship Between γ' Value and Its Angle to γ for Tremolite and Actinolite

Asbestos		Tremolite			Actinolite		
Apparent Extinction Angle (°)	Angle Between γ and γ' (°)	γ	γ'	$\gamma - \gamma''$	γ	γ'	$\gamma - \gamma''$
20*	0	1.6423	1.6423	0.0000	1.6485	1.6485	0.0000
19	1	1.6423	1.6423	0.0000	1.6485	1.6485	0.0000
18	2	1.6423	1.6423	0.0000	1.6485	1.6485	0.0000
17	3	1.6423	1.6422	0.0001	1.6485	1.6484	0.0001
16	4	1.6423	1.6422	0.0001	1.6485	1.6484	0.0001
15	5	1.6423	1.6421	0.0002	1.6485	1.6483	0.0002
14	6	1.6423	1.6420	0.0003	1.6485	1.6482	0.0003
13	7	1.6423	1.6418	0.0005	1.6485	1.6481	0.0004
12	8	1.6423	1.6417	0.0006	1.6485	1.6479	0.0006
11	9	1.6423	1.6416	0.0007	1.6485	1.6478	0.0007
10	10	1.6423	1.6414	0.0009	1.6485	1.6476	0.0009
9	11	1.6423	1.6412	0.0011	1.6485	1.6474	0.0011
8	12	1.6423	1.6410	0.0013	1.6485	1.6472	0.0013
7	13	1.6423	1.6408	0.0015	1.6485	1.6470	0.0015
6	14	1.6423	1.6405	0.0018	1.6485	1.6468	0.0017
5	15	1.6423	1.6403	0.0020	1.6485	1.6466	0.0019
4	16	1.6423	1.6400	0.0023	1.6485	1.6463	0.0022
3	17	1.6423	1.6397	0.0026	1.6485	1.6460	0.0025
2	18	1.6423	1.6394	0.0029	1.6485	1.6457	0.0028
1	19	1.6423	1.6391	0.0032	1.6485	1.6454	0.0031
0**	20	1.6423	1.6388	0.0035	1.6485	1.6451	0.0034

*True (maximum) extinction angle.
**Parallel extinction. γ' is the RI along the fiber elongation axis or c-axis.

Table 10. Converting Dispersion Staining Color to Corresponding λ_m (5)

Matching Wavelength λ_m[1], nm	Particle Edge Colors[2]		Becke Line Colors[3]	
	Annular Stop[4]	Central Stop[5]	Particle	Liquid
<340	Black violet	White	White	—
<400	Dark violet	Pale yellow	Pale yellow	—
430	Violet	Yellow	Pale yellow	—
455	Blue	Golden yellow	Yellow	Violet
485	Blue-green	Orange	Orange	Violet
520	Green	Red purple	Orange-red	Violet-blue
560	Yellow-green	Purple	Red-orange	Blue-violet
595	Yellow	Deep blue	Red	Blue
625	Orange	Blue-green	Faint red	Blue
660	Red-brown	Light blue-green	—	Blue-green
700	Dark red-brown	Pale blue-green	—	Pale blue-green
1500	Black-brown	Very pale blue-green	—	Very pale blue-green

[1]λ_0 in original table. [2]In focus.[3]On focusing up. [4]Observed on a brightfield. [5]Observed on a darkfield.

Table 11. Available λ_m and t to Asbestos RI Conversion Tables*

Asbestos	RI	DRIMMC	Cargille
Chrysotile	α	1.546 (HD-L)	1.545 (E)
	α and γ	1.550 (HD-S or L)	1.550 (E)
	γ	1.560 (HD-L)	1.560 (E)
Amosite	α	1.680 (HD-L)	1.680 (B)
	γ	1.700 (HD-L)	1.700 (B)
Crocidolite	α	1.700 (HD-L)	1.700 (B)
	γ	1.680 (HD-L)	1.680 (B)
Tremolite	α	1.605 (HD-L)	1.605 (E)
	γ	1.635 (HD-L)	1.635 (E)
	α and γ	1.620 (HD-L)	1.620 (E)
	α and γ	1.625 (HD-L)	1.625 (E)
Actinolite	α	1.605 (HD-L)	1.605 (E)
	γ	1.640 (HD-L)	1.640 (E)
	α and γ	1.620 (HD-L)	1.620 (E)
	α and γ	1.625 (HD-L)	1.625 (E)
Anthophyllite	α	1.605 (HD-L)	1.605 (E)
	γ	1.635 (HD-L)	1.635 (E)
	α and γ	1.620 (HD-L)	1.620 (E)
	α and γ	1.625 (HD-L)	1.625 (E)

*Download conversion tables by scanning the QR code at the end of this paper.

Table 12. Choice of Cargille Glass Set and Lot Number for RI Liquid Calibration

Nominal Liquid RI[1]	Nominal Glass RI[2]	M-7 Set	M-24 Set	M-25 Set	Remarks
1.550	1.550	C	D	D	M-24 and M-25 are the same.
1.605	1.600	B	C	C	All three sets are the same.
1.605	1.610	D	E	E	M-7 and M-24 are the same[3].
1.610	1.610	D	E	E	M-7 and M-24 are the same[3].
1.615	1.620	D	D	D	All three sets are the same.
1.620	1.620	C	D	D	M-24 and M-25 are the same.
1.625	1.625	B	C	C	M-24 and M-25 are the same.
1.630	1.625	B	C	C	M-24 and M-25 are the same.
1.635	1.640	C/D	D	C/D	M-7 and M-25 are the same[3].
1.640	1.640	C/D	D	C/D	M-7 and M-25 are the same[3].
1.680	1.680	C	C/D	C/D	All three sets are the same.
1.700	1.700	C	C/D	C/D	M-24 and M-25 are the same.

[1]On the bottle label. [2]On the vial label. [3]With different lot numbers.

Table 13. Calibration of DRIMMC 1.550 (HD-S or HD-L) Using Cargille Glass 1.55

λ_m (nm)	M7 Lot C (n_D = 1.55158)							M24 / M25 Lot D (n_D = 1.54801)						
	17° C	19° C	21° C	23° C	25° C	27° C	29° C	17° C	19° C	21° C	23° C	25° C	27° C	29° C
400	1.517	1.518	1.519	1.520	1.521	1.522	1.523	1.515	1.516	1.517	1.518	1.519	1.520	1.521
420	1.523	1.524	1.525	1.526	1.527	1.528	1.529	1.521	1.522	1.523	1.524	1.525	1.526	1.527
440	1.528	1.529	1.530	1.531	1.532	1.533	1.534	1.525	1.526	1.527	1.528	1.529	1.530	1.531
460	1.532	1.533	1.534	1.535	1.536	1.537	1.538	1.529	1.530	1.531	1.532	1.533	1.534	1.535
480	1.535	1.536	1.537	1.538	1.539	1.540	1.541	1.532	1.533	1.534	1.535	1.536	1.537	1.538
500	1.538	1.539	1.540	1.541	1.542	1.543	1.544	1.535	1.536	1.537	1.538	1.539	1.540	1.541
520	1.541	1.542	1.543	1.544	1.545	1.546	1.547	1.538	1.539	1.539	1.540	1.541	1.542	1.543
540	1.543	1.544	1.545	1.546	1.547	1.548	1.549	1.540	1.541	1.542	1.543	1.544	1.545	1.546
560	1.545	1.546	1.547	1.548	1.549	1.550	1.551	1.542	1.543	1.544	1.545	1.546	1.547	1.548
580	1.547	1.548	1.549	1.550	1.551	1.552	1.553	1.543	1.544	1.545	1.546	1.547	1.548	1.549
589	1.548	1.549	1.550	1.551	1.552	1.553	1.554	1.544	1.545	1.546	1.547	1.548	1.549	1.550
600	1.549	1.549	1.550	1.551	1.552	1.553	1.554	1.545	1.546	1.547	1.548	1.549	1.550	1.551
620	1.550	1.551	1.552	1.553	1.554	1.555	1.556	1.546	1.547	1.548	1.549	1.550	1.551	1.552
640	1.551	1.552	1.553	1.554	1.555	1.556	1.557	1.548	1.549	1.550	1.551	1.552	1.553	1.554
660	1.553	1.554	1.555	1.556	1.557	1.558	1.559	1.549	1.550	1.551	1.552	1.553	1.554	1.555
680	1.554	1.555	1.556	1.557	1.558	1.559	1.560	1.550	1.551	1.552	1.553	1.554	1.555	1.556
700	1.555	1.556	1.557	1.558	1.559	1.560	1.561	1.551	1.552	1.553	1.554	1.555	1.556	1.557
720	1.556	1.557	1.558	1.559	1.560	1.561	1.562	1.552	1.553	1.554	1.555	1.556	1.557	1.558
740	1.557	1.558	1.559	1.560	1.561	1.562	1.563	1.553	1.554	1.555	1.556	1.556	1.557	1.558
760	1.557	1.558	1.559	1.560	1.561	1.562	1.563	1.553	1.554	1.555	1.556	1.557	1.558	1.559
780	1.558	1.559	1.560	1.561	1.562	1.563	1.564	1.554	1.555	1.556	1.557	1.558	1.559	1.560
800	1.559	1.560	1.561	1.562	1.563	1.564	1.565	1.555	1.556	1.557	1.558	1.559	1.560	1.561

Table 14. Calibration of Cargille 1.550 (E) Using Cargille Glass 1.55

λ_m (nm)	M7 Lot C (n_D = 1.55158)							M24 / M25 Lot D (n_D = 1.54801)						
	17° C	19° C	21° C	23° C	25° C	27° C	29° C	17° C	19° C	21° C	23° C	25° C	27° C	29° C
400	1.518	1.519	1.520	1.521	1.522	1.523	1.524	1.516	1.517	1.518	1.519	1.520	1.521	1.522
420	1.523	1.524	1.525	1.526	1.527	1.528	1.529	1.521	1.522	1.523	1.524	1.525	1.526	1.527
440	1.528	1.529	1.530	1.531	1.532	1.533	1.534	1.525	1.526	1.527	1.528	1.529	1.530	1.531
460	1.532	1.533	1.534	1.535	1.536	1.537	1.538	1.529	1.530	1.531	1.532	1.533	1.534	1.535
480	1.535	1.536	1.537	1.538	1.539	1.540	1.541	1.532	1.533	1.534	1.535	1.536	1.537	1.538
500	1.538	1.539	1.540	1.541	1.542	1.543	1.544	1.535	1.536	1.537	1.538	1.539	1.540	1.541
520	1.541	1.542	1.543	1.544	1.545	1.546	1.547	1.538	1.539	1.540	1.541	1.542	1.543	1.544
540	1.543	1.544	1.545	1.546	1.547	1.548	1.549	1.540	1.541	1.542	1.543	1.544	1.545	1.546
560	1.545	1.546	1.547	1.548	1.549	1.550	1.551	1.542	1.543	1.544	1.545	1.546	1.547	1.548
580	1.547	1.548	1.549	1.550	1.551	1.552	1.553	1.543	1.544	1.545	1.546	1.547	1.548	1.549
589	1.548	1.549	1.550	1.551	1.552	1.553	1.554	1.544	1.545	1.546	1.547	1.548	1.549	1.550
600	1.549	1.550	1.550	1.551	1.552	1.553	1.554	1.545	1.546	1.547	1.548	1.549	1.550	1.551
620	1.550	1.551	1.552	1.553	1.554	1.555	1.556	1.546	1.547	1.548	1.549	1.550	1.551	1.552
640	1.551	1.552	1.553	1.554	1.555	1.556	1.557	1.548	1.549	1.550	1.551	1.551	1.552	1.553
660	1.553	1.554	1.555	1.555	1.556	1.557	1.558	1.549	1.550	1.551	1.552	1.553	1.554	1.555
680	1.554	1.555	1.556	1.557	1.558	1.559	1.560	1.550	1.551	1.552	1.553	1.554	1.555	1.556
700	1.555	1.556	1.557	1.558	1.559	1.560	1.561	1.551	1.552	1.553	1.554	1.555	1.556	1.557
720	1.556	1.557	1.558	1.559	1.560	1.561	1.562	1.552	1.553	1.554	1.555	1.556	1.557	1.558
740	1.557	1.558	1.558	1.559	1.560	1.561	1.562	1.552	1.553	1.554	1.555	1.556	1.557	1.558
760	1.557	1.558	1.559	1.560	1.561	1.562	1.563	1.553	1.554	1.555	1.556	1.557	1.558	1.559
780	1.558	1.559	1.560	1.561	1.562	1.563	1.564	1.554	1.555	1.556	1.557	1.558	1.559	1.560
800	1.559	1.560	1.561	1.562	1.563	1.564	1.565	1.555	1.556	1.557	1.558	1.559	1.560	1.561

Table 15. Parameters (n_D and Dispersion Coefficient) of DRIMMC and Cargille Liquids-Glass Combination Used in the Calculations of Lookup Conversion Tables

Liquid	Dispersion Coefficient		Glass	M-7 Set*			M-24 Set*			M-25 Set*		
n_D	DRIMMC	Cargille	ID	Lot	n_D	D.C.	Lot	n_D	D.C.	Lot	n_D	D.C.
1.545		0.0264	1.55	C	1.55158	0.01112	D	1.54801	0.01197	D	1.54801	0.01197
1.546	0.0266[a]		1.55	C	1.55158	0.01112	D	1.54801	0.01197	D	1.54801	0.01197
1.550	0.0274[b]	0.0267	1.55	C	1.55158	0.01112	D	1.54801	0.01197	D	1.54801	0.01197
1.550	0.0272[c]	0.0280	1.55	C	1.55158	0.01112	D	1.54801	0.01197	D	1.54801	0.01197
1.605	0.0313[d]	0.0243	1.61	D	1.61064	0.01076	E	1.61064	0.01076	E	1.61064	0.01076
1.610	0.0315[d]	0.0251	1.61	D	1.61064	0.01076	E	1.61064	0.01076	E	1.61064	0.01076
1.615	0.0318[d]	0.0259	1.62	C	1.61998	0.01708	D	1.62048	0.01708	D	1.62048	0.01708
1.620	0.0322[d]	0.0267	1.62	C	1.61998	0.01708	D	1.62048	0.01708	D	1.62048	0.01708
1.625	0.0325[d]	0.0275	1.625	B	1.62564	0.01759	C	1.62527	0.01756	C	1.62527	0.01756
1.630	0.0327[d]	0.0283	1.63	B	1.62564	0.01759	C	1.62527	0.01756	C	1.62527	0.01756
1.635	0.0331[d]	0.0291	1.64	C/D	1.64333	0.01343	D	1.63992	0.01066	C/D	1.64333	0.01343
1.640	0.0334[d]	0.0299	1.64	C/D	1.64333	0.01343	D	1.63992	0.01066	C/D	1.64333	0.01343
1.680	0.0361[a]	0.0348	1.68	D	1.67766	0.01223	C/D	1.67827	0.01226	C/D	1.67827	0.01226
1.680	0.0383[b]	0.0348	1.68	D	1.67766	0.01223	C/D	1.67827	0.01226	C/D	1.67827	0.01226
1.700	0.0378[b]	0.0370	1.70	C	1.70136	0.01709	C/D	1.70207	0.01710	C/D	1.70207	0.01710

*There is overlapping among the three sets of glasses. Different set and/or lot number may have the same n_D and dispersion coefficient.
[a]HD, [b]HD-L, [c]HD-S, [d]Average of HD and HD-L

Table 16. Form for Recording RI Liquid Calibration Results Using Cargille Glass Standards (18)

	RI Liquid Label	M-Set Cargille Glass Label		CSDS Observation of Glass		Liquid Temperature	Calibrated RI of Liquid	Absolute Difference	Accept or Reject	Initials of Analyst
Date	RI Value	RI value	Lot No.	Color	λ_m (nm)	t (°C)	$n_D^{25°C}$	8–2		
1	2	3	4	5	6	7	8	9	10	11
									A R	
									A R	
									A R	

1. Date.
2. The $n_D^{25°C}$ on the label of the RI liquid bottle.
3. The RI value on the label of Cargille glass vial (fill in the Set ID: 7, 24, or 25).
4. The lot number on the label of Cargille glass vial.
5. The predominant central stop dispersion staining color displayed by glass fragments.
6. The matching wavelength, λ_m, corresponding to the observed CSDS color in Column 5.
7. The temperature of the RI liquid or the room temperature if in equilibrium.
8. The reading based on the values in Columns 6 and 7 from the lookup conversion table for the liquid-glass combination, $n_D^{25°C}$, the calibrated RI of the liquid at 589 nm and 25° C.
9. Column 8 minus Column 2.
10. If the *absolute* value of Column 9 is less or equal to 0.004, circle A for *acceptable*; otherwise, circle R for *rejected*.
11. Analyst's initials.

THE MICROSCOPE • Vol. 69:2, pp 70–83, 2022

CRITICAL **FOCUS**

Brian J. Ford

The Cell Knows Who You Are

Can we alter our sexuality with a knife and a few chemicals? A sectioned rat fetus reminds us how we all truly began: as multicellular organisms with their own hard-wired identity.

My favorite slide is a rat fetus I sectioned as a student. This is such a revealing preparation. Everyone likes it — and everybody (absolutely everybody) points out its penis. The penis indicates at once that this is a male fetus — or at least, it did until recently. Now, transsexuals who are women but are desperate to be men, can have one created by a surgeon. Or can they? Of course not. You can no more fashion a fully functioning penis out of tissue than you can make a line-caught cod out of a tall tub of taramasalata. Men invading a women's racetrack or the privacy of their changing room are ineradicably men, no matter what tablets they take. It is the microscope which proves the point.

Organs aren't hunks of offal; the fabulous structures of which they are comprised develop from coordinated colonies of largely autonomous living cells that have taken millions of years to specialize. They are where your nature exists and where your sexuality resides. The body may be thought of as just a bag of organs (two of everything down the sides, one of everything down the middle), but those organs are incredibly complicated communities of cells, each working out what to do next. Science has done so much to understand where the organs are and what they're meant to do. We have picked the cells apart until we know where every type of molecule sits and how they are linked together. Yet there's a gigantic conceptual hole in the middle of all this: nobody understands what each cell actually does, how it lives its own individual life and communicates with its neighbors, how it works out what to do and how to live and when to die, and how it makes its own decisions dependent upon what's happening right now. Cells think. Cells work out their options. Cells adapt to changing situations. Yet people aren't told this — it's almost as if science hasn't noticed.

The joy of this rat section is not just that the organs are immediately recognizable, sure, but that the single cells within them can easily be seen. My interpretation of the living world — that multicellular organisms are best viewed as choreographed communities of separate cells — makes immediate sense simply because here we can discern the discrete cells and gauge a sense of scale. This fetus doesn't look like a plastic model. You can see that it's a complex community.

This fetus had set in a twisted orientation. Other students had rejected it — but to me it offered an unprecedented opportunity. It meant that, cut carefully on a microtome, we could visualize the important ventral anatomy (umbilicus, penis, and tail), while the off-center cut gave us a view of organs not seen in

The Selection of Cargille Immersion Liquids for Asbestos Analysis

Asbestos	RI	High Accuracy Required (Regulatory, litigation, forensic, etc.)	Routine Samples
Chrysotile	α	1.546/1.550 (E)	1.550 (E)
	γ	1.550/1.560 (E)	
Grunerite (Amosite)	α	1.680 (B)	1.680 (B)
	γ	1.700 (B)	
Riebeckite (Crocidolite)	α	1.700 (B)	1.680 (B)
	γ	1.680 (B)	
Tremolite	α	1.605/1.610/1.615 (E)	1.620 (E) 1.625 (E)
	γ	1.630/1.635 (E)	
Actinolite	α	1.605/1.610/1.615 (E)	
	γ	1.635/1.640 (E)	
Anthophyllite	α	1.605/1.610/1.615 (E)	
	γ	1.630/1.635/1.640 (E)	

2

Chrysotile

in Cargille 1.545 (E)

λ_m	α							γ						
(nm)	17°C	19°C	21°C	23°C	25°C	27°C	29°C	17°C	19°C	21°C	23°C	25°C	27°C	29°C
300	1.638	1.637	1.636	1.635	1.634	1.634	1.633	1.631	1.630	1.629	1.629	1.628	1.627	1.626
320	1.618	1.617	1.616	1.615	1.614	1.613	1.613	1.613	1.612	1.611	1.610	1.609	1.608	1.607
340	1.604	1.603	1.602	1.601	1.600	1.599	1.598	1.599	1.599	1.598	1.597	1.596	1.595	1.594
360	1.593	1.592	1.591	1.590	1.589	1.588	1.587	1.590	1.589	1.588	1.587	1.586	1.585	1.584
380	1.585	1.584	1.583	1.582	1.581	1.580	1.579	1.582	1.581	1.580	1.579	1.578	1.577	1.576
400	1.578	1.577	1.576	1.575	1.574	1.573	1.572	1.576	1.575	1.574	1.573	1.572	1.571	1.570
420	1.572	1.571	1.571	1.570	1.569	1.568	1.567	1.571	1.570	1.569	1.568	1.567	1.566	1.565
440	1.568	1.567	1.566	1.565	1.564	1.563	1.562	1.566	1.565	1.565	1.564	1.563	1.562	1.561
460	1.564	1.563	1.562	1.561	1.560	1.559	1.559	1.563	1.562	1.561	1.560	1.559	1.558	1.557
480	1.561	1.560	1.559	1.558	1.557	1.556	1.555	1.560	1.559	1.558	1.557	1.556	1.555	1.554
500	1.558	1.557	1.556	1.555	1.554	1.553	1.552	1.557	1.556	1.555	1.554	1.553	1.553	1.552
520	1.555	1.554	1.553	1.553	1.552	1.551	1.550	1.555	1.554	1.553	1.552	1.551	1.550	1.549
540	1.553	1.552	1.551	1.550	1.549	1.549	1.548	1.553	1.552	1.551	1.550	1.549	1.548	1.547
560	1.551	1.550	1.549	1.548	1.547	1.547	1.546	1.551	1.550	1.549	1.548	1.547	1.546	1.546
580	1.549	1.548	1.548	1.547	1.546	1.545	1.544	1.549	1.548	1.547	1.547	1.546	1.545	1.544
600	1.548	1.547	1.546	1.545	1.544	1.543	1.542	1.548	1.547	1.546	1.545	1.544	1.543	1.542
620	1.546	1.545	1.545	1.544	1.543	1.542	1.541	1.546	1.546	1.545	1.544	1.543	1.542	1.541
640	1.545	1.544	1.543	1.542	1.541	1.541	1.540	1.545	1.544	1.543	1.543	1.542	1.541	1.540
660	1.544	1.543	1.542	1.541	1.540	1.539	1.538	1.544	1.543	1.542	1.541	1.541	1.540	1.539
680	1.543	1.542	1.541	1.540	1.539	1.538	1.537	1.543	1.542	1.541	1.540	1.540	1.539	1.538
700	1.542	1.541	1.540	1.539	1.538	1.537	1.536	1.542	1.541	1.540	1.540	1.539	1.538	1.537
720	1.541	1.540	1.539	1.538	1.537	1.536	1.535	1.541	1.540	1.540	1.539	1.538	1.537	1.536
740	1.540	1.539	1.538	1.537	1.536	1.535	1.535	1.541	1.540	1.539	1.538	1.537	1.536	1.535
760	1.539	1.538	1.537	1.536	1.536	1.535	1.534	1.540	1.539	1.538	1.537	1.536	1.535	1.534
780	1.538	1.537	1.537	1.536	1.535	1.534	1.533	1.539	1.538	1.537	1.536	1.536	1.535	1.534
800	1.538	1.537	1.536	1.535	1.534	1.533	1.532	1.539	1.538	1.537	1.536	1.535	1.534	1.533
850	1.536	1.535	1.534	1.533	1.533	1.532	1.531	1.537	1.536	1.535	1.534	1.534	1.533	1.532
900	1.535	1.534	1.533	1.532	1.531	1.530	1.529	1.536	1.535	1.534	1.533	1.532	1.531	1.531
950	1.534	1.533	1.532	1.531	1.530	1.529	1.528	1.535	1.534	1.533	1.532	1.531	1.530	1.529
1000	1.533	1.532	1.531	1.530	1.529	1.528	1.527	1.534	1.533	1.532	1.531	1.530	1.529	1.529

Chrysotile

in Cargille 1.550 (E-Bulk Bottle)

λ_m	α							γ						
(nm)	17°C	19°C	21°C	23°C	25°C	27°C	29°C	17°C	19°C	21°C	23°C	25°C	27°C	29°C
300	1.648	1.647	1.646	1.645	1.644	1.643	1.642	1.641	1.640	1.639	1.638	1.637	1.636	1.635
320	1.627	1.626	1.625	1.624	1.623	1.622	1.621	1.622	1.621	1.620	1.619	1.618	1.617	1.616
340	1.612	1.611	1.610	1.609	1.608	1.607	1.606	1.608	1.607	1.606	1.605	1.604	1.603	1.602
360	1.600	1.599	1.599	1.598	1.597	1.596	1.595	1.597	1.596	1.595	1.594	1.593	1.592	1.591
380	1.592	1.591	1.590	1.589	1.588	1.587	1.586	1.589	1.588	1.587	1.586	1.585	1.584	1.583
400	1.585	1.584	1.583	1.582	1.581	1.580	1.579	1.582	1.581	1.580	1.579	1.578	1.578	1.577
420	1.579	1.578	1.577	1.576	1.575	1.574	1.573	1.577	1.576	1.575	1.574	1.573	1.572	1.571
440	1.574	1.573	1.572	1.571	1.570	1.569	1.568	1.573	1.572	1.571	1.570	1.569	1.568	1.567
460	1.570	1.569	1.568	1.567	1.566	1.565	1.564	1.569	1.568	1.567	1.566	1.565	1.564	1.563
480	1.567	1.566	1.565	1.564	1.563	1.562	1.561	1.566	1.565	1.564	1.563	1.562	1.561	1.560
500	1.564	1.563	1.562	1.561	1.560	1.559	1.558	1.563	1.562	1.561	1.560	1.559	1.558	1.557
520	1.561	1.560	1.559	1.558	1.557	1.556	1.555	1.560	1.559	1.558	1.557	1.557	1.556	1.555
540	1.559	1.558	1.557	1.556	1.555	1.554	1.553	1.558	1.557	1.556	1.555	1.554	1.553	1.552
560	1.557	1.556	1.555	1.554	1.553	1.552	1.551	1.556	1.555	1.554	1.553	1.552	1.551	1.550
580	1.555	1.554	1.553	1.552	1.551	1.550	1.549	1.555	1.554	1.553	1.552	1.551	1.550	1.549
600	1.553	1.552	1.551	1.550	1.549	1.548	1.547	1.553	1.552	1.551	1.550	1.549	1.548	1.547
620	1.552	1.551	1.550	1.549	1.548	1.547	1.546	1.552	1.551	1.550	1.549	1.548	1.547	1.546
640	1.550	1.549	1.548	1.547	1.546	1.545	1.544	1.550	1.549	1.548	1.547	1.547	1.546	1.545
660	1.549	1.548	1.547	1.546	1.545	1.544	1.543	1.549	1.548	1.547	1.546	1.545	1.544	1.543
680	1.548	1.547	1.546	1.545	1.544	1.543	1.542	1.548	1.547	1.546	1.545	1.544	1.543	1.542
700	1.547	1.546	1.545	1.544	1.543	1.542	1.541	1.547	1.546	1.545	1.544	1.543	1.542	1.541
720	1.546	1.545	1.544	1.543	1.542	1.541	1.540	1.546	1.545	1.544	1.543	1.542	1.541	1.540
740	1.545	1.544	1.543	1.542	1.541	1.540	1.539	1.545	1.545	1.544	1.543	1.542	1.541	1.540
760	1.544	1.543	1.542	1.541	1.540	1.539	1.538	1.545	1.544	1.543	1.542	1.541	1.540	1.539
780	1.543	1.542	1.541	1.540	1.539	1.538	1.537	1.544	1.543	1.542	1.541	1.540	1.539	1.538
800	1.542	1.542	1.541	1.540	1.539	1.538	1.537	1.543	1.542	1.541	1.540	1.539	1.538	1.537
850	1.541	1.540	1.539	1.538	1.537	1.536	1.535	1.542	1.541	1.540	1.539	1.538	1.537	1.536
900	1.539	1.538	1.538	1.537	1.536	1.535	1.534	1.541	1.540	1.539	1.538	1.537	1.536	1.535
950	1.538	1.537	1.536	1.535	1.534	1.533	1.532	1.539	1.538	1.537	1.536	1.535	1.534	1.534
1000	1.537	1.536	1.535	1.534	1.533	1.532	1.531	1.538	1.537	1.536	1.535	1.535	1.534	1.533

Chrysotile

in Cargille 1.550 (E-Set)

λ_m	α							γ						
(nm)	17°C	19°C	21°C	23°C	25°C	27°C	29°C	17°C	19°C	21°C	23°C	25°C	27°C	29°C
300	1.653	1.652	1.651	1.650	1.649	1.648	1.647	1.646	1.645	1.644	1.643	1.642	1.641	1.640
320	1.630	1.629	1.628	1.627	1.626	1.625	1.624	1.625	1.624	1.623	1.622	1.621	1.620	1.619
340	1.615	1.614	1.613	1.612	1.611	1.610	1.609	1.610	1.609	1.608	1.607	1.606	1.605	1.604
360	1.603	1.602	1.601	1.600	1.599	1.598	1.597	1.599	1.598	1.597	1.596	1.595	1.594	1.593
380	1.594	1.593	1.592	1.591	1.590	1.589	1.588	1.591	1.590	1.589	1.588	1.587	1.586	1.585
400	1.586	1.585	1.584	1.583	1.582	1.581	1.580	1.584	1.583	1.582	1.581	1.580	1.579	1.578
420	1.580	1.579	1.578	1.577	1.576	1.575	1.574	1.578	1.577	1.576	1.575	1.574	1.573	1.572
440	1.575	1.574	1.573	1.572	1.571	1.570	1.569	1.574	1.573	1.572	1.571	1.570	1.569	1.568
460	1.571	1.570	1.569	1.568	1.567	1.566	1.565	1.570	1.569	1.568	1.567	1.566	1.565	1.564
480	1.567	1.566	1.565	1.564	1.563	1.562	1.561	1.566	1.565	1.564	1.563	1.562	1.561	1.560
500	1.564	1.563	1.562	1.561	1.560	1.559	1.558	1.563	1.562	1.561	1.560	1.559	1.558	1.557
520	1.561	1.560	1.559	1.558	1.557	1.556	1.555	1.561	1.560	1.559	1.558	1.557	1.556	1.555
540	1.559	1.558	1.557	1.556	1.555	1.554	1.553	1.559	1.558	1.557	1.556	1.555	1.554	1.553
560	1.557	1.556	1.555	1.554	1.553	1.552	1.551	1.556	1.556	1.555	1.554	1.553	1.552	1.551
580	1.555	1.554	1.553	1.552	1.551	1.550	1.549	1.555	1.554	1.553	1.552	1.551	1.550	1.549
600	1.553	1.552	1.551	1.550	1.549	1.548	1.547	1.553	1.552	1.551	1.550	1.549	1.548	1.547
620	1.551	1.550	1.549	1.548	1.547	1.546	1.546	1.552	1.551	1.550	1.549	1.548	1.547	1.546
640	1.550	1.549	1.548	1.547	1.546	1.545	1.544	1.550	1.549	1.548	1.547	1.546	1.545	1.544
660	1.549	1.548	1.547	1.546	1.545	1.544	1.543	1.549	1.548	1.547	1.546	1.545	1.544	1.543
680	1.547	1.546	1.546	1.545	1.544	1.543	1.542	1.548	1.547	1.546	1.545	1.544	1.543	1.542
700	1.546	1.545	1.544	1.543	1.542	1.541	1.540	1.547	1.546	1.545	1.544	1.543	1.542	1.541
720	1.545	1.544	1.543	1.542	1.541	1.540	1.539	1.546	1.545	1.544	1.543	1.542	1.541	1.540
740	1.544	1.543	1.542	1.541	1.540	1.539	1.538	1.545	1.544	1.543	1.542	1.541	1.540	1.539
760	1.544	1.543	1.542	1.541	1.540	1.539	1.538	1.544	1.543	1.542	1.541	1.540	1.539	1.538
780	1.543	1.542	1.541	1.540	1.539	1.538	1.537	1.543	1.543	1.542	1.541	1.540	1.539	1.538
800	1.542	1.541	1.540	1.539	1.538	1.537	1.536	1.543	1.542	1.541	1.540	1.539	1.538	1.537
850	1.540	1.539	1.538	1.537	1.536	1.535	1.534	1.541	1.540	1.539	1.538	1.537	1.536	1.535
900	1.539	1.538	1.537	1.536	1.535	1.534	1.533	1.540	1.539	1.538	1.537	1.536	1.535	1.534
950	1.538	1.537	1.536	1.535	1.534	1.533	1.532	1.539	1.538	1.537	1.536	1.535	1.534	1.533
1000	1.536	1.535	1.534	1.533	1.532	1.531	1.531	1.538	1.537	1.536	1.535	1.534	1.533	1.532

Chrysotile

in Cargille 1.560 (E)

λ_m (nm)	α 17°C	α 19°C	α 21°C	α 23°C	α 25°C	α 27°C	α 29°C	γ 17°C	γ 19°C	γ 21°C	γ 23°C	γ 25°C	γ 27°C	γ 29°C
300	1.652	1.651	1.650	1.649	1.648	1.647	1.646	1.645	1.644	1.643	1.642	1.641	1.641	1.640
320	1.632	1.631	1.630	1.629	1.628	1.628	1.627	1.627	1.626	1.625	1.624	1.623	1.622	1.621
340	1.618	1.617	1.616	1.615	1.614	1.613	1.613	1.614	1.613	1.612	1.611	1.610	1.609	1.608
360	1.607	1.606	1.606	1.605	1.604	1.603	1.602	1.604	1.603	1.602	1.601	1.600	1.599	1.599
380	1.599	1.598	1.597	1.596	1.595	1.595	1.594	1.596	1.595	1.595	1.594	1.593	1.592	1.591
400	1.593	1.592	1.591	1.590	1.589	1.588	1.587	1.590	1.589	1.588	1.588	1.587	1.586	1.585
420	1.587	1.586	1.585	1.584	1.583	1.583	1.582	1.585	1.584	1.583	1.583	1.582	1.581	1.580
440	1.583	1.582	1.581	1.580	1.579	1.578	1.577	1.581	1.580	1.579	1.578	1.577	1.577	1.576
460	1.579	1.578	1.577	1.576	1.575	1.574	1.573	1.578	1.577	1.576	1.575	1.574	1.573	1.572
480	1.576	1.575	1.574	1.573	1.572	1.571	1.570	1.575	1.574	1.573	1.572	1.571	1.570	1.569
500	1.573	1.572	1.571	1.570	1.569	1.568	1.567	1.572	1.571	1.570	1.569	1.568	1.567	1.567
520	1.570	1.569	1.568	1.567	1.567	1.566	1.565	1.570	1.569	1.568	1.567	1.566	1.565	1.564
540	1.568	1.567	1.566	1.565	1.564	1.563	1.563	1.568	1.567	1.566	1.565	1.564	1.563	1.562
560	1.566	1.565	1.564	1.563	1.562	1.562	1.561	1.566	1.565	1.564	1.563	1.562	1.561	1.560
580	1.564	1.563	1.563	1.562	1.561	1.560	1.559	1.564	1.563	1.562	1.562	1.561	1.560	1.559
600	1.563	1.562	1.561	1.560	1.559	1.558	1.557	1.563	1.562	1.561	1.560	1.559	1.558	1.557
620	1.561	1.560	1.560	1.559	1.558	1.557	1.556	1.562	1.561	1.560	1.559	1.558	1.557	1.556
640	1.560	1.559	1.558	1.557	1.556	1.556	1.555	1.560	1.559	1.559	1.558	1.557	1.556	1.555
660	1.559	1.558	1.557	1.556	1.555	1.554	1.553	1.559	1.558	1.557	1.557	1.556	1.555	1.554
680	1.558	1.557	1.556	1.555	1.554	1.553	1.552	1.558	1.557	1.556	1.556	1.555	1.554	1.553
700	1.557	1.556	1.555	1.554	1.553	1.552	1.551	1.557	1.556	1.556	1.555	1.554	1.553	1.552
720	1.556	1.555	1.554	1.553	1.552	1.551	1.550	1.557	1.556	1.555	1.554	1.553	1.552	1.551
740	1.555	1.554	1.553	1.552	1.551	1.551	1.550	1.556	1.555	1.554	1.553	1.552	1.551	1.550
760	1.554	1.553	1.552	1.552	1.551	1.550	1.549	1.555	1.554	1.553	1.552	1.551	1.550	1.550
780	1.554	1.553	1.552	1.551	1.550	1.549	1.548	1.554	1.553	1.553	1.552	1.551	1.550	1.549
800	1.553	1.552	1.551	1.550	1.549	1.548	1.547	1.554	1.553	1.552	1.551	1.550	1.549	1.548
850	1.551	1.550	1.550	1.549	1.548	1.547	1.546	1.552	1.551	1.550	1.550	1.549	1.548	1.547
900	1.550	1.549	1.548	1.547	1.546	1.546	1.545	1.551	1.550	1.549	1.548	1.547	1.547	1.546
950	1.549	1.548	1.547	1.546	1.545	1.544	1.543	1.550	1.549	1.548	1.547	1.546	1.546	1.545
1000	1.548	1.547	1.546	1.545	1.544	1.543	1.542	1.549	1.548	1.547	1.546	1.546	1.545	1.544

Amosite

in Cargille 1.680 (B)

λ_m	α							γ						
(nm)	17°C	19°C	21°C	23°C	25°C	27°C	29°C	17°C	19°C	21°C	23°C	25°C	27°C	29°C
300	1.765	1.764	1.763	1.762	1.761	1.760	1.759	1.765	1.764	1.763	1.762	1.761	1.760	1.759
320	1.747	1.746	1.745	1.744	1.743	1.742	1.741	1.747	1.746	1.745	1.744	1.743	1.742	1.741
340	1.734	1.733	1.732	1.731	1.730	1.729	1.728	1.734	1.733	1.732	1.731	1.730	1.729	1.728
360	1.724	1.723	1.722	1.721	1.720	1.719	1.718	1.724	1.723	1.722	1.721	1.720	1.719	1.718
380	1.716	1.715	1.714	1.713	1.713	1.712	1.711	1.716	1.715	1.714	1.713	1.713	1.712	1.711
400	1.710	1.709	1.708	1.707	1.706	1.706	1.705	1.710	1.709	1.708	1.707	1.706	1.706	1.705
420	1.705	1.704	1.703	1.702	1.702	1.701	1.700	1.705	1.704	1.703	1.702	1.702	1.701	1.700
440	1.701	1.700	1.699	1.698	1.697	1.696	1.695	1.701	1.700	1.699	1.698	1.697	1.696	1.695
460	1.698	1.697	1.696	1.695	1.694	1.693	1.692	1.698	1.697	1.696	1.695	1.694	1.693	1.692
480	1.695	1.694	1.693	1.692	1.691	1.690	1.689	1.695	1.694	1.693	1.692	1.691	1.690	1.689
500	1.692	1.691	1.690	1.689	1.688	1.687	1.686	1.692	1.691	1.690	1.689	1.688	1.687	1.686
520	1.690	1.689	1.688	1.687	1.686	1.685	1.684	1.690	1.689	1.688	1.687	1.686	1.685	1.684
540	1.688	1.687	1.686	1.685	1.684	1.683	1.682	1.688	1.687	1.686	1.685	1.684	1.683	1.682
560	1.686	1.685	1.684	1.683	1.682	1.681	1.680	1.686	1.685	1.684	1.683	1.682	1.681	1.680
580	1.684	1.683	1.683	1.682	1.681	1.680	1.679	1.684	1.683	1.683	1.682	1.681	1.680	1.679
600	1.683	1.682	1.681	1.680	1.679	1.678	1.677	1.683	1.682	1.681	1.680	1.679	1.678	1.677
620	1.682	1.681	1.680	1.679	1.678	1.677	1.676	1.682	1.681	1.680	1.679	1.678	1.677	1.676
640	1.681	1.680	1.679	1.678	1.677	1.676	1.675	1.681	1.680	1.679	1.678	1.677	1.676	1.675
660	1.679	1.679	1.678	1.677	1.676	1.675	1.674	1.679	1.679	1.678	1.677	1.676	1.675	1.674
680	1.678	1.678	1.677	1.676	1.675	1.674	1.673	1.678	1.678	1.677	1.676	1.675	1.674	1.673
700	1.678	1.677	1.676	1.675	1.674	1.673	1.672	1.678	1.677	1.676	1.675	1.674	1.673	1.672
720	1.677	1.676	1.675	1.674	1.673	1.672	1.671	1.677	1.676	1.675	1.674	1.673	1.672	1.671
740	1.676	1.675	1.674	1.673	1.672	1.671	1.670	1.676	1.675	1.674	1.673	1.672	1.671	1.670
760	1.675	1.674	1.673	1.672	1.671	1.671	1.670	1.675	1.674	1.673	1.672	1.671	1.671	1.670
780	1.675	1.674	1.673	1.672	1.671	1.670	1.669	1.675	1.674	1.673	1.672	1.671	1.670	1.669
800	1.674	1.673	1.672	1.671	1.670	1.669	1.668	1.674	1.673	1.672	1.671	1.670	1.669	1.668
850	1.673	1.672	1.671	1.670	1.669	1.668	1.667	1.673	1.672	1.671	1.670	1.669	1.668	1.667
900	1.671	1.670	1.669	1.669	1.668	1.667	1.666	1.671	1.670	1.669	1.669	1.668	1.667	1.666
950	1.670	1.669	1.668	1.667	1.667	1.666	1.665	1.670	1.669	1.668	1.667	1.667	1.666	1.665
1000	1.669	1.668	1.668	1.667	1.666	1.665	1.664	1.669	1.668	1.668	1.667	1.666	1.665	1.664